
Article:
Liu, X., Cederwall, B., Qi, C. et al. (2022) Evidence for spherical-oblate shape coexistence in Tc 87. Physical Review C. 034304. ISSN: 2469-9993

https://doi.org/10.1103/PhysRevC.106.034304

Evidence for spherical-oblate shape coexistence in ^{87}Tc

X. Liu,[1,2,3,*] B. Cederwall,[1] C. Qi,[1] R. A. Wyss,[1] Ö. Aktas,[1] A. Ertoprak,[1,4] W. Zhang,[1] E. Clément,[5] G. de France,[5] D. Ralet,[6] A. Gadea,[7] A. Goasduff,[8] G. Jaworski,[8,9] I. Kuti,[10] B. M. Nyakó,[10] J. Nyberg,[11] M. Palacz,[9] R. Wadsworth,[12] J. J. Valiente-Dobón,[8] H. Al-Azri,[13] A. Ataç Nyberg,[1] T. Bäck,[1] G. de Angelis,[8] M. Doncel,[14,15] J. Dudouet,[16] A. Gottardo,[6] M. Jurado,[7] J. Ljungvall,[6] D. Mengoni,[8] D. R. Napoli,[8] C. M. Petrache,[17] D. Sohler,[10] J. Timár,[10] D. Barrientos,[18] P. Bednarczyk,[19] G. Benzoni,[20] B. Birkenbach,[21] A. J. Boston,[14] H. C. Boston,[14] I. Burrows,[22] L. Charles,[23] M. Ciemala,[19] F. C. L. Crespi,[24,20] D. M. Cullen,[25] P. Désesquelles,[26,6] C. Domingo-Pardo,[7] J. Eberth,[21] N. Erduran,[27] S. Ertürk,[28] V. González,[29] J. Goupil,[5] H. Hess,[21] T. Huyuk,[7] A. Jungclaus,[30] W. Korten,[31] A. Lemasson,[5] S. Leoni,[24,20] A. Maj,[19] R. Menegazzo,[32] B. Million,[20] R. M. Perez-Vidal,[7] Zs. Podolyàk,[33] A. Pullia,[24,20] F. Recchia,[32] P. Reiter,[21] F. Saillant,[5] M. D. Salsac,[31] E. Sanchis,[29] J. Simpson,[22] O. Stezowski,[16] C. Theisen,[31] and M. Zielińska[31]

[1]*Department of Physics, Royal Institute of Technology, Stockholm 104 05, Sweden*
[2]*Institute of Modern Physics, Chinese Academy of Sciences, Lanzhou 730000, China*
[3]*University of Chinese Academy of Sciences, Beijing 100049, China*
[4]*Department of Physics, Faculty of Science, Istanbul University, Vezneciler/Fatih, 34134 Istanbul, Turkey*
[5]*GANIL, CEA/DRF-CNRS/IN2P3, Boulevard Henri Becquerel, BP 55027, F-14076 Caen Cedex 5, France*
[6]*Centre de Sciences Nucléaires et Sciences de la Matière, CNRS/IN2P3, Université Paris-Saclay, 91405 Orsay, France*
[7]*Instituto de Fìsica Corpuscular, CSIC-Universidad de Valencia, E-46980 Valencia, Spain*
[8]*Istituto Nazionale di Fisica Nucleare, Laboratori Nazionali di Legnaro, I-35020 Legnaro, Italy*
[9]*Heavy Ion Laboratory, University of Warsaw, ul. Pasteura 5A, 02-093 Warszawa, Poland*
[10]*Institute for Nuclear Research, Atomki, H-4001 Debrecen, Hungary*
[11]*Department of Physics and Astronomy, Uppsala University, SE-75121 Uppsala, Sweden*
[12]*Department of Physics, University of York, Heslington, York YO10 5DD, United Kingdom*
[13]*Department of Mathematical & Physical Sciences, University of Nizwa, Sultanate of Oman*
[14]*Oliver Lodge Laboratory, The University of Liverpool, Liverpool L69 7ZE, United Kingdom*
[15]*Department of Physics, Stockholm University, Stockholm 106 91, Sweden*
[16]*Université Lyon, CNRS/IN2P3, IPN-Lyon, F-69622, Villeurbanne, France*
[17]*Université Paris-Saclay, CNRS/IN2P3, IJCLab, 91405 Orsay, France*
[18]*CERN, CH-1211 Geneva 23, Switzerland*
[19]*The Henryk Niewodniczański Institute of Nuclear Physics, Polish Academy of Sciences, ul. Radzikowskiego 152, 31-342 Kraków, Poland*
[20]*INFN Milano, I-20133 Milano, Italy*
[21]*Institut für Kernphysik, Universität zu Köln, Zülpicher Straße 77, D-50937 Köln, Germany*
[22]*STFC Daresbury Laboratory, Daresbury, Warrington WCNRS 4AD, United Kingdom*
[23]*IPHC, UNISTRA, CNRS, 23 Rue du Loess, 67200 Strasbourg, France*
[24]*Department of Physics, University of Milano, I-20133 Milano, Italy*
[25]*Nuclear Physics Group, Schuster Laboratory, University of Manchester, Manchester M13 9PL, United Kingdom*
[26]*CNRS-IN2P3, Université Paris-Saclay, Bat 104, F-91405 Orsay Campus, France*
[27]*Faculty of Engineering and Natural Sciences, Istanbul Sabahattin Zaim University, 34303 Istanbul, Turkey*
[28]*Department of Physics, University of Nigde, 51240 Nigde, Turkey*
[29]*Departamento de Ingenierìa Electrònica, Universitat de Valencia, 46100 Burjassot, Valencia, Spain*
[30]*Instituto de Estructura de la Materia, CSIC, Madrid, E-28006 Madrid, Spain*
[31]*IRFU, CEA, Université Paris-Saclay, F-91191 Gif-sur-Yvette, France*
[32]*INFN Padova, I-35131 Padova, Italy*
[33]*Department of Physics, University of Surrey, Guildford GU2 7XH, United Kingdom*

(Received 10 September 2021; revised 24 January 2022; accepted 23 March 2022; published 9 September 2022)

Excited states in the neutron-deficient nucleus ^{87}Tc have been studied via the fusion-evaporation reaction ^{54}Fe(^{36}Ar, $2n1p$)^{87}Tc at 115 MeV beam energy. The AGATA γ-ray spectrometer coupled to the DIAMANT, NEDA, and Neutron Wall detector arrays for light-particle detection was used to measure the prompt coincidence

*xiaoyuli@kth.se

of γ rays and light particles. Six transitions from the deexcitation of excited states belonging to a new band in ^{87}Tc were identified by comparing γ-ray intensities in the spectra gated under different reaction channel selection conditions. The constructed level structure was compared with the shell model and total Routhian surface calculations. The results indicate that the new band structure in ^{87}Tc is built on a spherical configuration, which is different from that assigned to the previously identified oblate yrast rotational band.

DOI: 10.1103/PhysRevC.106.034304

I. INTRODUCTION

Nuclei in the vicinity of the $N = Z$ line with $A \geqslant 80$ have been the subject of intense study in recent years. Of special interest in this region of the Segrè chart, lying between the strongly deformed nucleus ^{76}Sr [1,2] and the doubly magic nucleus ^{100}Sn, are the predictions of shape transitions and shape coexistence [3,4], as well as the possible effects of enhanced neutron-proton pairing correlations [5]. Major difficulties in the experimental study of this remote area close to the proton drip line are the low production cross sections and the limited number of stable beam-target combinations that can be used for fusion-evaporation reactions, which has made the experimental progress increasingly challenging. One example of recent experimental advancements is the study of the level structure of the heaviest deformed self-conjugate nucleus ^{88}Ru [6,7], for which the yrast ground-state band was extended, including the observation of the first backbending [8]. Another example is the yrast band in the $N = Z + 1$ nucleus ^{87}Tc, for which two previously known γ-ray transitions [9] were recently extended to a rotational band structure [10].

We here report on the identification of new excited states in ^{87}Tc populated in the fusion-evaporation reaction ^{54}Fe(^{36}Ar, $2n1p$)^{87}Tc. The prompt γ rays were assigned to the $2n1p$ channel by comparing the intensities of γ rays in the spectra gated under different reaction channel selection conditions. The constructed level structure is discussed within the framework of shell model and total Routhian surface calculations.

II. EXPERIMENT

The experiment was performed at the Grand Accélérateur National d'Ions Lourds (GANIL). The fusion-evaporation reaction ^{54}Fe(^{36}Ar, $2n1p$)^{87}Tc was induced by a 115 MeV ^{36}Ar beam bombarding the 6 mg/cm^2 thick, isotopically enriched (99.58%) metallic ^{54}Fe target (0.40% ^{56}Fe, 0.015% ^{57}Fe, and 0.005% ^{58}Fe). Prompt γ rays emitted in the reaction were detected by the Advanced GAmma Tracking Array (AGATA) in its GANIL implementation [11] consisting of 11 triple-cluster segmented high-purity germanium (HPGe) detectors [12]. Energy and efficiency calibration of the AGATA detectors were performed with a ^{152}Eu standard radioactive source giving a 0.095% σ/E (1.3 keV) resolution for the 1408.1 keV transition. The detection of emitted light particles for the channel selection was achieved by the DIAMANT, NEDA, and Neutron Wall arrays. Evaporated charged particles were measured by the DIAMANT [13,14] array consisting of 60 CsI(Tl) scintillators placed inside the target chamber. The NEDA [15,16] and Neutron Wall [17] neutron detector arrays, consisting of 54 and 42 organic liquid scintillator detectors, respectively, were placed in the forward hemisphere with respect to the beam, covering approximately 1.6π solid angle in the laboratory system. The event trigger condition required at least two different AGATA detectors represented by different crystals to fire in coincidence with at least one neutron detector (NEDA or Neutron Wall) to record a neutron-like event.

During the ten-day experiment with a beam intensity of 5–10 p nA, about 2×10^{10} reaction events fulfilling the trigger condition were collected. In the offline analysis, prompt γ rays were sorted into different γ-γ coincidence matrices according to the detected light particles. The DIAMANT charged particle detectors were placed in the forward hemisphere resulting in single-proton detection efficiency of 39(1)% [and α detection efficiency of 35(1)%]. Therefore, both the $0p$- and $1p$- gated events were used in the analysis to increase the statistics. The requirement of $01p$ events was either a complete silence of the whole DIAMANT array or the presence of a signal assigned to a proton. The probability of neutron scattering between detectors was relatively high due to the geometry of the NEDA and Neutron Wall. To suppress the contamination from the $1n$-related channels in the $2n$-gated γ-ray energy spectra, a purification of the $2n$ events was performed to reject the scattering events by using the time-of-flight of the detected neutrons and the positions of the fired detectors [18]. A comparison of $2n$-gated spectra before and after the purification is shown in Fig. 1. Under the described selection condition, approximately 1.9×10^7 reaction events were sorted into the final $2n01p$ γ-γ coincidence matrix. Due to trigger requirements, the neutron detection efficiency cannot be measured reliably. The simulation of the setup [15] shows that the $1n$ and $2n$ detection efficiency is about 15% and 2% respectively. The experimental cross section of ^{87}Tc was estimated to be approximately 280 μb.

III. RESULTS

Based on the present experiment, we previously extended the yrast band of ^{87}Tc in Ref. [10] [see Fig. 2(c) on the basis of the reported 712 and 887 keV transitions [9]. In this study, the weaker reported γ-ray cascade was subsequently identified, and assigned to the $2n1p$ channel by comparing the γ-ray intensities in the spectra gated under different channel selection conditions. Figures 2(a) and 2(b) show coincidence spectra from the $2n01p$ γ-γ coincidence matrix, in which all six newly identified transitions, 718.6(1), 731.6(2), 791.7(2), 862.8(1), 905(1), and 1042.4(4) keV, are clearly visible.

The ratio between γ-ray intensities measured in spectra gated under different particle multiplicity conditions depends

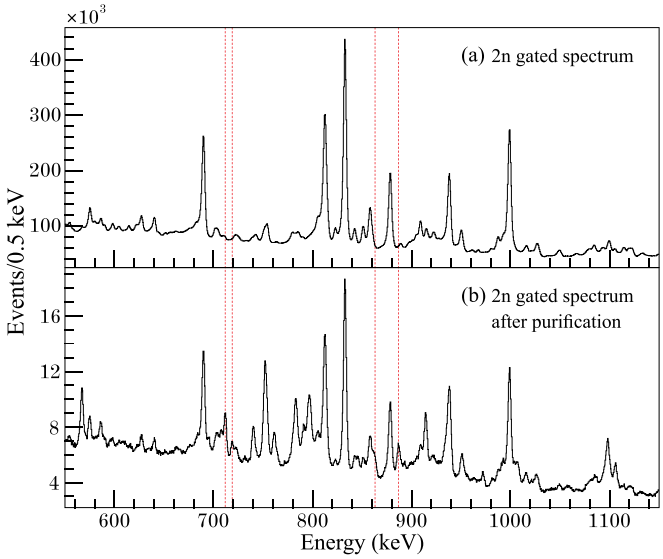

FIG. 1. Comparison of the total $2n$-gated spectrum (a) and the $2n$-gated spectrum after the purification (b). The enhanced and new peaks in the spectrum (b) come from $2n$ related channels. The four red dotted lines indicate the positions of the 712, 887, 719, and 863 keV peaks from ^{87}Tc.

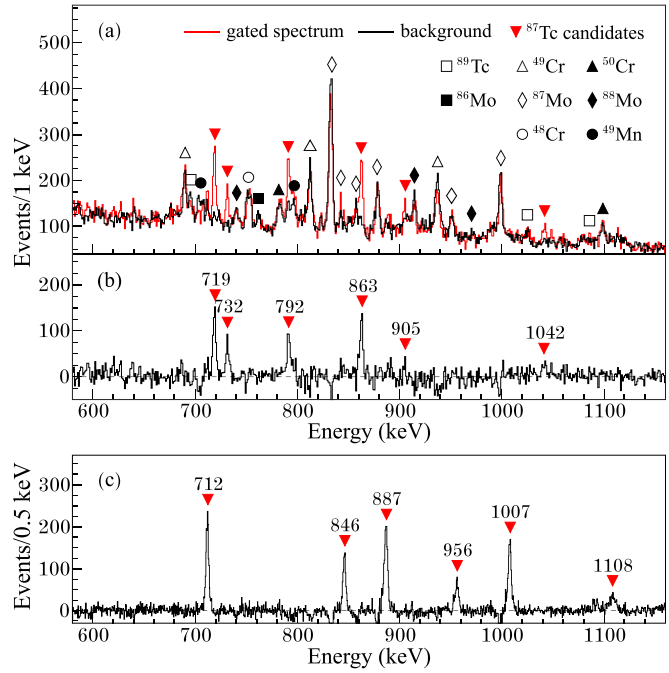

FIG. 2. For the newly identified γ rays, (a) sum of the gated spectra (red) on 718.6, 731.6, 791.7, 862.8, 905, and 1042.4 keV lines with the width of 2 keV, and summed normalized background spectra (black) gated 4.75 keV above these lines with the width of 2.5 keV. The coincidence spectrum in (b) is the difference between the two spectra in (a). For the previously reported yrast band, (c) sum of the background-subtracted coincidence spectra for the yrast band in ^{87}Tc [10] gated on the 712.0, 886.5, 1007.4, 845.9, and 956.3 keV lines.

on the detection efficiencies for the particles and the reaction channel of the specific transition. In addition to impurities from heavy iron isotopes, the ^{54}Fe target foils used in the experiment were also contaminated by ^{16}O due to oxidation from the residual O_2 in the beam-line vacuum, accelerated by beam-induced heating of the target. The γ rays of the fusion-evaporation products resulting from ^{36}Ar beam bombardment of target impurities, such as ^{49}Mn [21] [from ^{16}O(^{36}Ar, $2n1p$)^{49}Mn] and ^{89}Tc [22] [from ^{56}Fe(^{36}Ar, $2n1p$)^{89}Tc], were used as references for the channel assignment of the observed transitions. In Fig. 3, the intensity ratios between transitions in the $1p2n$-gated and the $0p2n$-gated spectra are shown. The intensity ratios for all the six new ^{87}Tc candidates are consistent with those of the known $1p$ evaporation channels. In addition, we confirmed that these lines are not present in the $1\alpha 2n$-gated and the $2p2n$-gated spectra. These results unambiguously identify the six γ rays as belonging to a $1p$-evaporation channel. The γ-ray intensity ratios in spectra from different neutron gates are shown in Fig. 4, from which we can conclude that the six new transitions are from a $2n$-related channel.

For the $2n1p$ channel, only three nuclei, ^{49}Mn, ^{89}Tc, and ^{87}Tc, were produced in the experiment in any significant amounts. ^{49}Mn can be excluded based on its relatively large cross section and the existing γ-ray spectroscopy of ^{49}Mn [21] and its mirror ^{49}Cr [19]. In the newly discovered cascade, there is a transition at 791.7 keV, the energy of which is close to the two known transitions in ^{89}Tc at 791 and 792 keV [22,23]. In the $2n01p$ matrix, the 791.7 keV line can coincide with the transitions from both ^{89}Tc and the new cascade, but no ^{89}Tc transition is visible in the spectra when gated on other members of the new cascade (see Fig. 5). This excludes the new cascade from belonging to ^{89}Tc, since it would reasonably have been discovered in the γ-γ coincidence analysis of the previous study [22]. Based on the above discussion, we assigned the new cascade to ^{87}Tc. Figure 5 also reflects the coincidence relationships between the γ rays with energies 719, 863, 792, 732, and 1042 keV, while the 905 keV transition only coincides with the 719 and 863 keV transitions. A level scheme, established based on the

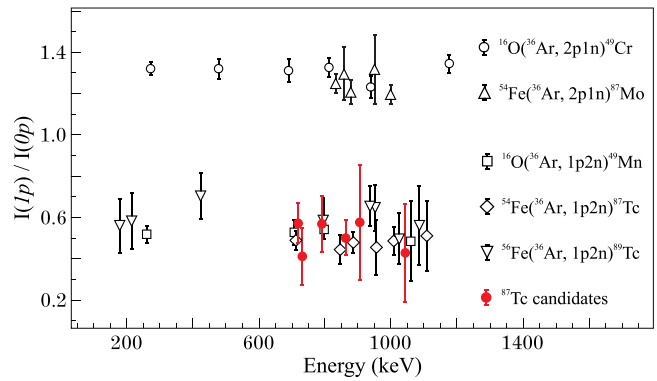

FIG. 3. Intensity ratios for different γ-ray transitions deduced from the $1p$-gated spectrum and the $0p$-gated spectrum. All ratios were measured using other coincident transitions as gates. The transition energies of ^{49}Cr and ^{87}Mo are from Ref. [19,20].

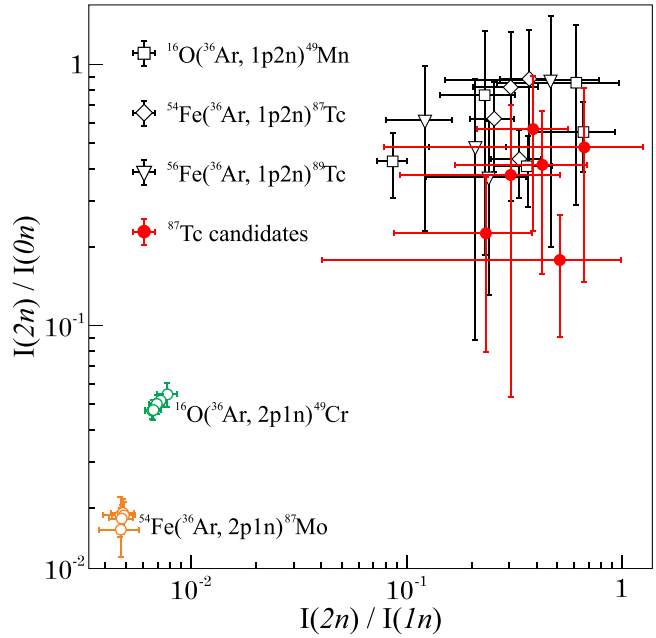

FIG. 4. Intensity ratios for different γ-ray transitions deduced from the 0n-gated spectrum, the 1n-gated spectrum, and the 2n-gated spectrum. In the measurement, triple γ-γ-γ coincidences are used for a better peak-to-background ratio.

coincidence relationships and the relative intensities of the γ rays listed in Table I, is displayed in Fig. 6. Due to the limited angular coverage of AGATA for DCO measurement, tentative spin-parity assignments were made based on the results of shell-model calculations (see below). In the present experiment, no transition connecting the observed cascade and the

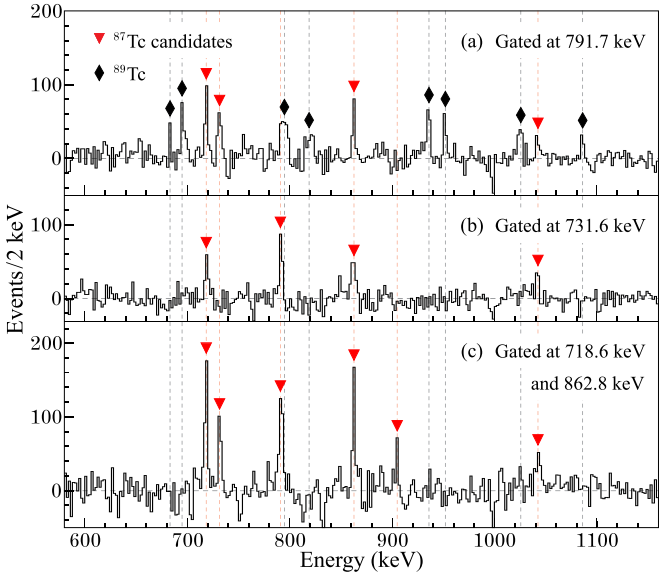

FIG. 5. The background-subtracted spectra gated at 791.7 keV (a), 731.6 keV (b), 718.6 and 862.8 keV (c). The width of all gates was 3 keV. The background spectra were gated in the range from 3 to 18 keV above these lines, excluding all areas covered by clear peaks in these energy intervals.

TABLE I. The γ-ray transition energies in keV (E_γ) and the relative intensities (I_{rel}). The upper part of the table is for the new cascade while the lower part is for the yrast band [10]. ×3 indicates that the intensity ratio between the transitions at 712 and 863 keV is approximately 3.0(3).

E_γ	I_{rel}	E_γ	I_{rel}
862.8(1)	100(10)	731.6(2)	32(7)
718.6(1)	87(9)	905(1)	12(4)
791.7(2)	57(8)	1042.4(4)	18(5)
712.0(1)	100(4) × 3	845.9(1)	37(4) × 3
886.5(1)	80(3) × 3	956.3(2)	26(3) × 3
1007.4(1)	65(5) × 3	1108.1(4)	13(3) × 3

previously identified yrast band in ^{87}Tc [10] was identified. The intensity of the 712 keV transition, corresponding to the lowest $(13/2^+_1) \rightarrow (9/2^+_1)$ transition in the yrast band, is approximately three times higher than that of the 863 keV transition in the newly observed cascade.

IV. DISCUSSION

The low-lying level structure of neutron deficient $N = 44$ isotones shows rotational-like behavior, as can be inferred from the known experimental data [10,24–27]. In ^{85}Nb and ^{83}Y [24–27], the negative parity bands with different signatures are linked by relatively strong $E2/M1$ transitions, while the positive-parity bands are dominated by stretched $E2$

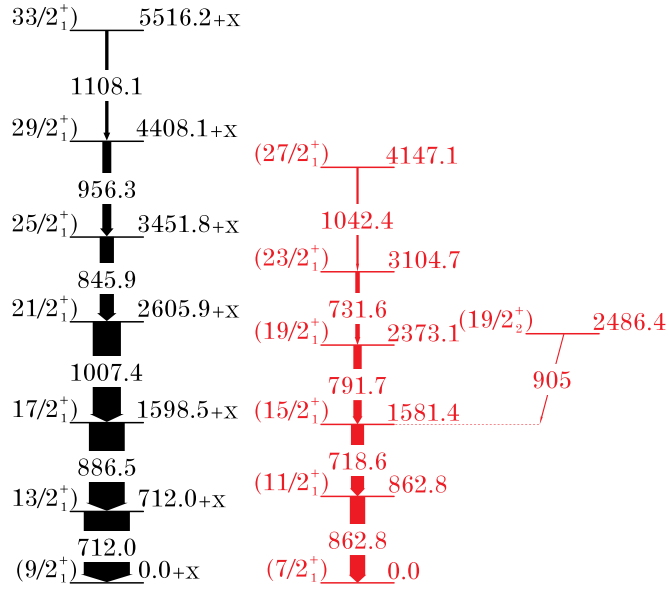

FIG. 6. Level scheme of ^{87}Tc. The left part (black) is for the yrast band from Ref. [10]. The right part (red) is deduced in the present work. The width of the arrows are proportional to the relative intensities of the γ rays listed in Table I. Based on TRS calculations, we propose the newly discovered $(7/2^+_1)$ state as the ground state, and the $(9/2^+_1)$ state reported in Ref. [10] as the excited state. "+X" in the left part is used to indicate an overall shift due to the unknown excitation energy of the $(9/2^+_1)$ state.

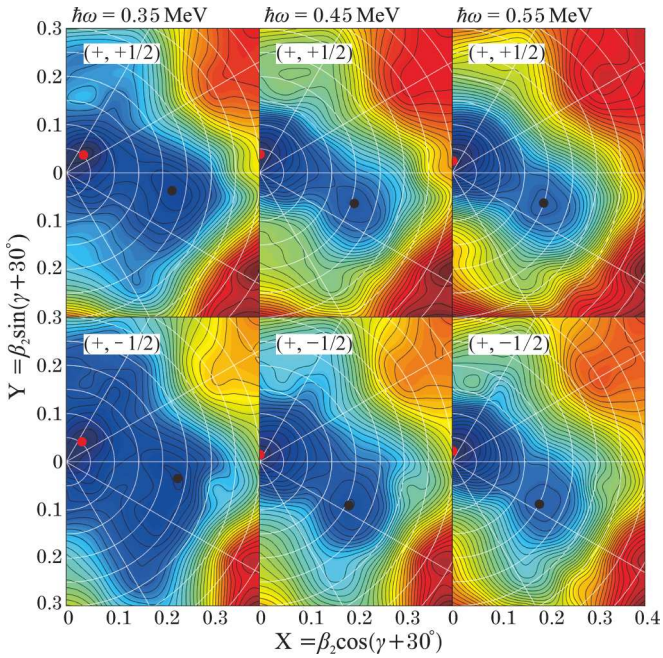

FIG. 7. Total Routhian surfaces in the (β_2, γ) plane for the $(\pi, \alpha) = (+, +1/2)$ and $(+, -1/2)$ configurations in ^{87}Tc. The distance between contour lines is 0.2 MeV. The positions of spherical and oblate minima on the surfaces are marked with red and black dots, respectively.

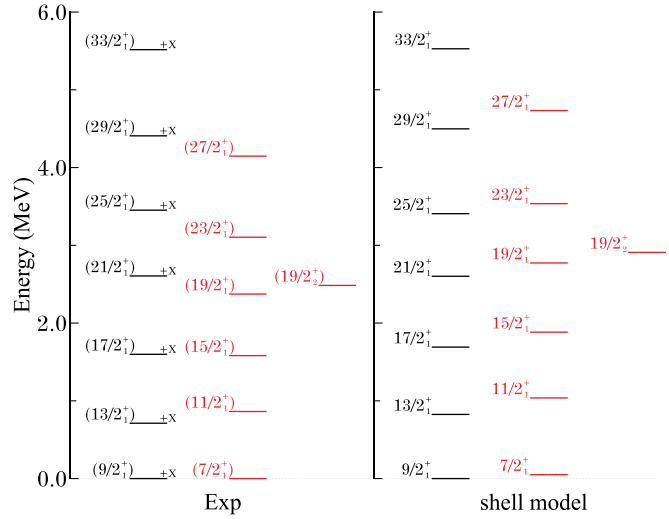

FIG. 8. Comparison of the experimental level scheme (left) and the shell model prediction (right).

transitions. The γ-ray cascade identified in the present work is structurally more similar to the positive parity bands from the systematics of excitation energies.

Total Routhian surface (TRS) calculations, which employ a deformed Wood-Saxon potential with monopole and quadrupole pairing residual interactions for different configurations as a function of the cranking frequency [28], were carried out for ^{87}Tc to study the deformation and spin alignment of the yrast states. Among the four calculated configurations (parity, signature) = $(\pi = \pm, \alpha = \pm 1/2)$, the Routhians of the positive-parity configurations are lower (at least 700 keV). The corresponding surfaces in the (β_2, γ) plane are displayed in Fig. 7. Deformed minima, all associated with a transition from a soft near-triaxial minimum $(0.22, -40^\circ)$ to a near-oblate more rigid shape $(0.20, -48^\circ)$, reflect a $g_{9/2}$ neutron alignment around $\hbar\omega = 0.45$ MeV. This structure is assigned to the previously identified yrast band [10]. The calculated alignment frequency is similar to the experimental observation, and the proposed deformation is close to Möller's prediction [3] of an oblate ground state in ^{87}Tc with $\beta_2 \approx -0.24$. The near-oblate deformation is induced by particle-hole excitations of neutrons and protons from the fp shell to the $1g_{9/2}$ substates. The calculation predicts the negative-signature configuration to lie somewhat higher in energy and the minimum is softer. The newly observed irregular level structure assigned to ^{87}Tc does not exhibit a rotational behavior. The shape of these states could be spherical corresponding to the spherical minima as shown in Fig. 7. The spherical minimum in the surface is predicted to be the lowest in the full rotational frequency range up to $\hbar\omega = 0.55$ MeV and hence to form the ground-state band.

A shell model calculation for the positive-parity states in ^{87}Tc was performed with the slgmt0 interaction [29] in a configuration space consisting of $2p_{1/2}$ and $1g_{9/2}$ orbitals for protons and neutrons. A comparison between the known experimental level structure of ^{87}Tc and the shell-model predictions is shown in Fig. 8. For the positive signature band (black) built on the $(9/2^+_1)$ state [10], the shell model calculation provides a good description above 2.6 MeV excitation energy, while the collectivity below the $(21/2^+_1)$ state appears underestimated which may be due to the limitation of valence space. The red one built on the $7/2^+_1$ state has a overall match with the newly observed level structure. Although the calculated level energies are higher, the ratios of transition energies $R_1 = E_\gamma(15/2^+ \rightarrow 11/2^+)/E_\gamma(11/2^+ \rightarrow 7/2^+)$ from the experiment (0.83) and the calculation (0.85) are similar, and both values are lower than the rotational (1.40) and vibrational (1.0) limits, indicating a noncollective structure.

The calculated energy differences between the predicted $9/2^+_1$ and $7/2^+_1$ states (50 keV) are within the model uncertainties. Hence, we can not rule out the possibility that the $7/2^+_1$ state actually forms the spherical ground state as suggested by the TRS calculation.

V. CONCLUSIONS

In summary, we have studied the low-lying excited states of ^{87}Tc via the ^{54}Fe(^{36}Ar, $2n1p$)^{87}Tc fusion-evaporation reaction at the GANIL accelerator complex. The AGATA γ-ray spectrometer was used in conjunction with the DIAMANT, NEDA, and Neutron Wall detector arrays to measure the prompt coincidences of γ rays, neutrons, and charged particles. Six new γ-ray transitions, with energies at 718.6(1), 731.6(2), 791.7(2), 862.8(1), 905(1), and 1042.4(4) keV, were identified by means of comparison of γ-ray intensities in the spectra gated under different channel selection

conditions. The observed cascade contains no transition linking to the known yrast band of ^{87}Tc. The constructed states were tentatively assigned to positive parity, and the results were compared with shell model and TRS calculations. The proposed level structure exhibits spherical behavior different from the yrast band which is assigned to an oblate-deformed shape.

ACKNOWLEDGMENTS

This work was supported by the Swedish Research Council under Grants No. 621-2014-5558 and No. 2019-04880; the EU 7th Framework Programme, Integrating Activities Transnational Access, Project No. 262010 ENSAR; the UK STFC under Grants No. ST/L005727/1 and No. ST/P003885/1; the Polish National Science Centre, Grants No. 2016/22/M/ST2/00269 and No. 2017/25/B/ST2/01569; COPIN-INFN, COPIN-IN2P3, and COPIGAL projects; the National Research, Development and Innovation Fund of Hungary (Project No. K128947); the European Regional Development Fund (Contract No. GINOP-2.3.3-15-2016-00034); the Hungarian National Research, Development and Innovation Office, NKFIH, Contract No. PD124717; the Ministerio de Ciencia e Innovación and Generalitat Valenciana, Spain, under the Grants No. SEV-2014-0398 and No. FPA2017-84756-C4; PROMETEO/2019/005; and by the EU FEDER funds. X.L. gratefully acknowledges support from the China Scholarship Council, Grant No. 201700260183, for his stay in Sweden. We acknowledge the support from the AGATA Collaboration and thank the GANIL staff for excellent technical support and operation.

[1] B. J. Varley *et al.*, Phys. Lett. B **194**, 463 (1987).
[2] C. J. Lister, P. J. Ennis, A. A. Chishti, B. J. Varley, W. Gelletly, H. G. Price, and A. N. James, Phys. Rev. C **42**, R1191 (1990).
[3] P. Möller, A. J. Sierk, T. Ichikawa, and H. Sagawa, At. Data Nucl. Data Tables **109-110**, 1 (2016).
[4] D. Bucurescu, C. Rossi Alvarez, C. A. Ur, N. Marginean, P. Spolaore, D. Bazzacco, S. Lunardi, D. R. Napoli, M. Ionescu-Bujor, A. Iordachescu, C. M. Petrache, G. deAngelis, A. Gadea, D. Foltescu, F. Brandolini, G. Falconi, E. Farnea, S. M. Lenzi, N. H. Medina, Z. Podolyak, M. DePoli, M. N. Rao, and R. Venturelli, Phys. Rev. C **56**, 2497 (1997).
[5] S. Frauendorf and A. Macchiavelli, Prog. Part. Nucl. Phys. **78**, 24 (2014).
[6] N. Mărginean, C. Rossi Alvarez, D. Bucurescu, C. A. Ur, A. Gadea, S. Lunardi, D. Bazzacco, G. deAngelis, M. Axiotis, M. DePoli, E. Farnea, M. Ionescu-Bujor, A. Iordachescu, S. M. Lenzi, T. Kroll, T. Martinez, R. Menegazzo, D. R. Napoli, G. Nardelli, P. Pavan, B. Quintana, and P. Spolaore, Phys. Rev. C **63**, 031303(R) (2001).
[7] N. Mărginean, D. Bucurescu, C. RossiAlvarez, C. A. Ur, Y. Sun, D. Bazzacco, S. Lunardi, G. deAngelis, M. Axiotis, E. Farnea, A. Gadea, M. Ionescu-Bujor, A. Iordachescu, W. Krolas, T. Kroll, S. M. Lenzi, T. Martinez, R. Menegazzo, D. R. Napoli, P. Pavan, Z. Podolyak, M. DePoli, B. Quintana, and P. Spolaore, Phys. Rev. C **65**, 051303(R) (2002).
[8] B. Cederwall *et al.*, Phys. Rev. Lett. **124**, 062501 (2020).
[9] D. Rudolph *et al.*, J. Phys. G: Nucl. Part. Phys. **17**, L113 (1991).
[10] X. Liu *et al.*, Phys. Rev. C **104**, L021302 (2021).
[11] E. Clément *et al.*, Nucl. Instrum. Methods Phys. Res., Sect. A **855**, 1 (2017).
[12] S. Akkoyun *et al.*, Nucl. Instrum. Methods Phys. Res., Sect. A **668**, 26 (2012).
[13] J. Scheurer *et al.*, Nucl. Instrum. Methods Phys. Res., Sect. A **385**, 501 (1997).
[14] J. Gál *et al.*, Nucl. Instrum. Methods Phys. Res., Sect. A **516**, 502 (2004).
[15] T. Hüyük *et al.*, Eur. Phys. J. A **52**, 55 (2016).
[16] J. J. Valiente-Dobón *et al.*, Nucl. Instrum. Methods Phys. Res., Sect. A **927**, 81 (2019).
[17] O. Skeppstedt *et al.*, Nucl. Instrum. Methods Phys. Res., Sect. A **421**, 531 (1999).
[18] X. Liu, Experimental studies of the neutron deficient atomic nuclei ^{88}Ru and ^{87}Tc, and the diagonalization of general pairing hamiltonian, Doctoral Thesis in Physics, KTH Royal Institute of Technology, 2021 (unpublished).
[19] J. A. Cameron, M. A. Bentley, A. M. Bruce, R. A. Cunningham, W. Gelletly, H. G. Price, J. Simpson, D. D. Warner, and A. N. James, Phys. Rev. C **44**, 1882 (1991).
[20] Ch. Winter *et al.*, Nucl. Phys. A **535**, 137 (1991).
[21] J. A. Cameron *et al.*, Phys. Lett. B **235**, 239 (1990).
[22] D. Rudolph *et al.*, Nucl. Phys. A **587**, 181 (1995).
[23] D. Rudolph *et al.*, Z. Phys. A: Hadrons Nucl. **342**, 121 (1992).
[24] K. Jonsson *et al.*, Nucl. Phys. A **645**, 47 (1999).
[25] C. J. Gross *et al.*, Nucl. Phys. A **535**, 203 (1991).
[26] T. D. Johnson, A. Aprahamian, C. J. Lister, D. Blumenthal, B. Crowell, P. Chowdury, P. Fallon, and A. Machiavelli, Phys. Rev. C **55**, 1108 (1997).
[27] F. Cristancho *et al.*, Nucl. Phys. A **540**, 307 (1992).
[28] W. Satula and R. Wyss, Phys. Scr. **T56**, 159 (1995).
[29] F. J. D. Serduke, R. D. Lawson, and D. H. Gloeckner, Nucl. Phys. A **256**, 45 (1976).